A Fast Fourier Transform Spectrometer design for submillimeter site testing.

Miguel Velázquez.[a] Daniel Ferrusca[a] and David H. Hughes.[a]

[a]INAOE, Luis E. Erro No. 1, Tonantzintla, México

ABSTRACT

We report the design of a sub-millimeter Fourier Transform Spectrometer of the Martin Puplett type (FTS-MP here after). The instrument will be installed on Sierra La Negra, and will operate from ∼215 GHz to 1 THz approximately with a moderate resolution of 500 MHz. The main motivations of the work are the development of basic instrumentation for characterizing the LMT site (Large Millimeter Telescope) as well as optical components and to provide a portable broadband system for site testing. The collected data will be used for transmission model validation. The data also will influence the design of the new generation of sub-millimeter and millimeter cameras for the LMT. In the present work we emphasize cryogenic detector system design (bolometer detector and coupling optics) and the optical system layout for the FTS-MP. Test measurements in the laboratory are reported in this work.

Keywords: FTS, Martin-Puplett interferometer, Site testing, LMT

1. INTRODUCTION

The submillimetre and millimetre wavelength range (here after sub-mm) is part of the electromagnetic spectrum which remains almost unexplored. The sub-mm astronomy is a young field that focuses mainly on the study of cool thermal sources (e.g. interstellar dust ∼ 10 K, which has a blackbody emission that peaks at 300 μm, such material is strongly related with early evolutionary stages of galaxies, starts and planets). However, the atmosphere at sub-mm wavelengths is partially transparent. Pressure broadened transitions of the atmospheric molecules contribute to the opacity at sub-mm wavelengths, mainly water vapor, which absorbs and emits radiation. The above produce inherent noise in the reception system, as well as, attenuates the astronomical signal. Therefore the atmospheric water content is the primary cause of opacity, hence ground-based observation is best performed from sites which have an atmosphere with low water vapor content and very high temporal stability.

Continuous radiometric (at 215 GHz) atmospheric opacity measurements[1, 2]at LMT site made since 1997, have provided data which demonstrates the feasible sub-mm ground-based observations, due to large fraction of the year (November through May) the median of the opacity is 0.2 or less. These information just reflect the narrow band behavior of the sky, hence a better understand of the broadband characteristics is necessary because the main technology in sub-mm is dominated by broadband detectors (i.e bolometer arrays like AZTEC, SPEED etc.), which require optical filtering in order to work in a specific band. Nevertheless, heterodyne receivers (i.e. SEQUOIA, Z-machine, etc.) are benefited for broadband characterization, that information allows to design optimally the band of operation. To provide broadband information of the atmospheric opacity from ∼215 GHz to 1 THz, we have designed and built a Fourier Transform Spectrometer of the Martin Puplett type which is planned to be installed at the summit of Sierra La Negra.

The FTS-MP has a linear translation stage with a useful travel of 18 cm, which allows to have a resolution up to ∼ 0.5 GHz (neglecting the finite aperture of the system). This resolution is enough to measure the profile of the atmospheric windows as well as to resolve some spectral issues (e.g. water vapor emission). The pressure broadened of the water vapor line shapes obtained from the FTS-MP will provide a measurement of the water vapor content.

Further author information: (Send correspondence to M.V.)
M.V.: E-mail: miyang@inaoep.mx, Telephone: + 52 222 266 31 00 ext. 1120
D.F: E-mail: dferrus@inaoep.mx, Telephone: + 52 222 266 31 00 ext. 1120

Millimeter and Submillimeter Detectors and Instrumentation for Astronomy III,
edited by Jonas Zmuidzinas, Wayne S. Holland, Stafford Withington, William D. Duncan,
Proc. of SPIE Vol. 6275, 627521, (2006) · 0277-786X/06/$15 · doi: 10.1117/12.684617

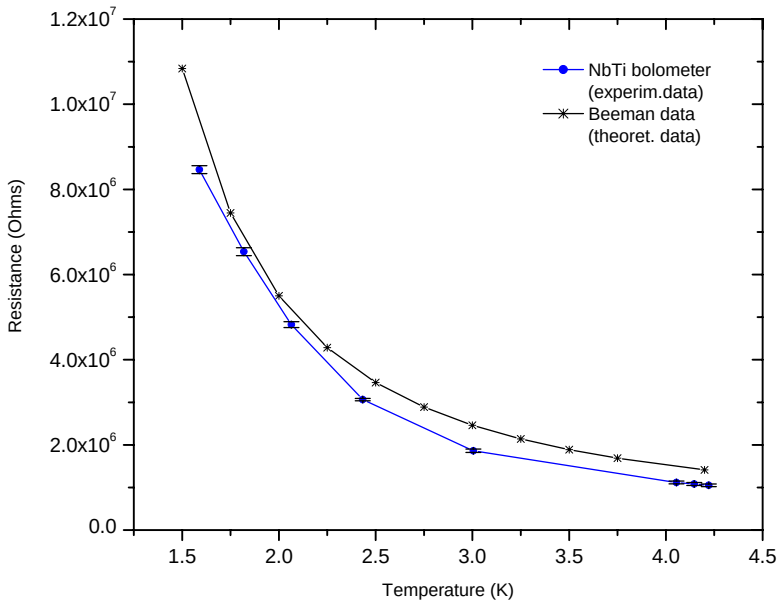

Figure 1. Experimental R-T curve for NTD type B thermistor compared with theoretical data. There is 10-20% systematic offset between the experimental and theoretical data, this is expected since the epoxy that glues the thermistor to the absorber produces a slight stress on the chip which may change its resistance from the ideal thermistor.

2. DETECTION SYSTEM

The FTS-MP will detect radiation in a band from ∼300 μm (i.e. limit imposed by the optics of the FTS-MP) to ∼1.4 mm (i.e. limit of the entrance aperture of the feedhorn) which will result in an integrated power P∼22 nW. In order to be able to detect this power we have designed a composite bolometer[3] with a thermal conductance G=5.47×10^{-8} W/K , NEP$_G$=1.20×10^{-14} W/Hz$^{1/2}$ and a responsivity S=1.83 MV/K. Detailed theory a can be found elsewhere.[4, 5]

2.1. Composite Bolometer for the FTS-MP

In the FTS-MP instrument, we use a composite bolometer which has a small semiconductor element, with a large temperature coefficient of resistance, mounted on a dielectric substrate. The semiconductor serves as a thermometer to measure the changes in temperature while the dielectric substrate serves as the absorber of the incident radiation.

The bolometer has a thermistor, which is a small cube (250 μm per side) of nuclear transmutation doped germanium[6] (NTD Ge type B). The thermistor follows the expression $R_{Bol}=R^*\exp(T_G/T)^{1/2}$ (see figure 1), where T_G=52.30 K and R^*=30.5 KΩ have been found experimentally. The thermistor is mounted on a thin sapphire disk and it is coated with 0.1μm of bismuth on the opposite side of the absorber material to improve the absorption efficiency. The absorber element is thermally coupled to a low temperature bath through two 12 μm niobium titanium wires which also serve as electrical wires, and is mechanically supported by a polymer material (nylon). The thermistor is bonded to the absorber with a thermal epoxy. The nylon and NbTi wires are supported in a metallic ring, with electrical connections that allows the bolometer to be installed and interchanged without damage.

Radiation is coupled to the bolometer via a Winston horn light-collector which has the maximum theoretical concentration ratio.[7] The Winston horn (or feedhorn) cavity is gold-plated to improve the efficiency, which is highly dependent on the smoothness of the reflecting surface. The feedhorn has an entrance aperture of 10.16 mm and an exit aperture of 1.4 mm which defines a collecting angle of ∼12 degrees.

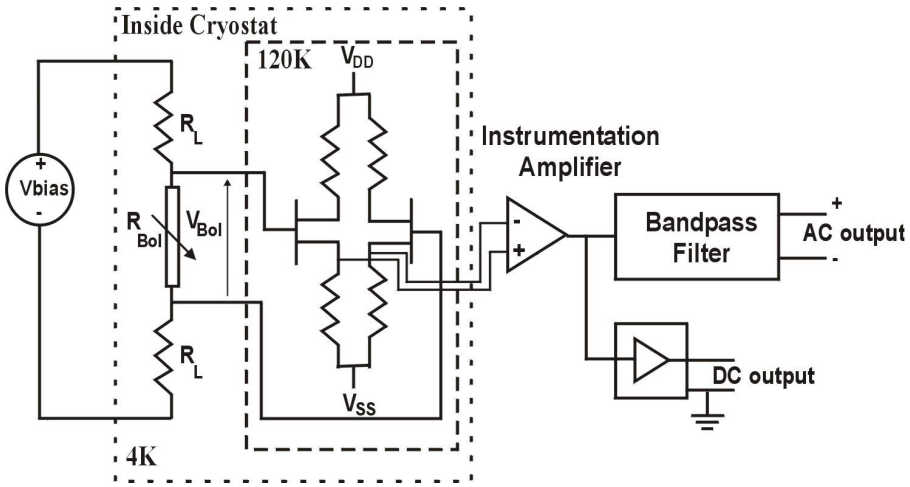

Figure 2. Schematic diagram of bolometer readout.

2.2. Detector bias and readout

The bolometer is in series with two 10 MΩ metal film resistors which are close to the bolometer at the bath temperature to minimize the Johnson noise contributions. The configuration is DC voltage biased. The bolometer modulated signal (using an external chopper) is sent to the SST/U401 dual JFET from Siliconix. JFET's are used on the first stage of amplification as a source follower to transform the high bolometer impedance into a low-source impedance. The JFET's are close to the bolometer to reduce microphonic pick up, and operate at ∼ 120K to reduce gate current noise, thus requiring thermal isolation from the cold plate.

The JFET's signals are sent to a room temperature preamplifier which consists of two stages. The first stage is a precision instrumentation amplifier (INA114 from Burr Brown) which is used to amplify the small differential signal across the bolometer and reject common-mode noise. It is configured as an AC coupled amplifier with four external selectable gains (1, 2, 5 and 10). This configuration provides the DC voltage across the bolometer and an AC channel output. The second stage is an active biquad bandpass filter (OP-270 from Analog Devices) with a gain of ∼2.5. Figure 2 shows an schematic diagram of the stages described above.

The output from the warm amplifier is sent to a lock-in amplifier to demodulate the signal and finally is digitized using a DAQ board (from National Instruments).

2.3. Cryogenic System

The performance of the bolometer has been tested in ^{4}He Oxford Instruments cryostat. The cryostat consists of an outer layer at room temperature which act as vacuum chamber, a liquid nitrogen shield (77 K), a vapor shield (∼40 K), and the liquid ^{4}He cold-plate (∼4 K). The radiation shields minimize the thermal loading on the cold stage. The LN_2 and ^{4}He vessels are wrapped with layers of super insulation material made of reflective aluminized Mylar thermally isolated from each other by a nylon mesh to improve the effectiveness of the shields, thus reducing radiation heat leak and heat transfer.

The LN_2 vessel is a 4.5 liter stainless steel tank, suspended from the top plate by three fiberglass supports and three fill tubes, to which is attached a thin aluminum 77 K shield. The ^{4}He vessel has a capacity of 4 liters and a hold time of ∼48 hours (by pumping-down directly the vessel). Pumping on the liquid ^{4}He allows the cold plate to reach a temperature of ∼1.49 to 1.9 K. The ^{4}He vessel is mounted on the bottom of the LN_2 tank, supported by 3 more fiberglass rods. A vapor shield extends from the liquid ^{4}He vessel creating a 40 K shield. At the base of the ^{4}He vessel is the gold-plated copper cold-plate, which serves as the mounting surface for the optics, JFET's, the bolometer and its connections. The temperatures within the dewar are monitored with diode thermometers (DT470) and readout with a temperature monitor (Lake Shore Inc., model 128).

3. POLARIZING FTS

The FTS is a polarizing interferometer of the Martin Puplett type.[8] Table 1 summarizes the configuration of the FTS-MP. Since commercially available FTS systems are expensive and not focused on astronomical applications, the FTS-MP was developed in our laboratory. A block diagram of the FTS-MP is showed in figure 3. The interferometer has two input ports which are defined by the polarizer P1. One input port views the source (e.g. blackbody source, the sky, etc.) which is modulated against cold load source (LN $\sim$ 77 K) by a chopper. The other input port views the reference load at known temperature ($\sim$ 300 K). The reference loads consists in a millimeter wave absorbing material (ECOSSORB) at both ambient and liquid nitrogen temperature (the absorber is sunk into a liquid nitrogen reservoir covered with thin polyethylene to prevent rapid evaporation of the liquid nitrogen). The Martin-Puplett interferometer allows two output ports but in our system the polarizer P2 is set for a single output. The beam splitter BS and the polarizers P1, P2 are wire-grid polarizers of 25μm tungsten wire, with 75 μm period. The interfered beam is focused by the mirror PM2 into a Winston horn feeding a NTD Ge composite bolometer. The interferogram is recorded by driving at constant velocity the roof-mirror M2, the lag step size is defined by the sampling rate of the data acquisition system. The sampling rate can be changed in order to have different frequency resolution. The typical integration time at constant velocity of 40 μ/s is 6 minutes. The FTS-MP is mounted on an optical bench, enclosed with an acrylic box, which is purged with nitrogen gas. This minimizes adsorption within the FTS-MP and prevents condensation on the cryostat window.

The linear stage has a high accuracy lead screw driven by a servo motor and the position along the track is provided by the control system of the servo motor (Animatics, SmartMotor). Because the long wavelengths involved, no additional feedback system (i.e. secondary He-Ne interferometer) is required to control the position. All the functions, including bolometer signal digitization, motor control and thermometry are performed by a personal computer.

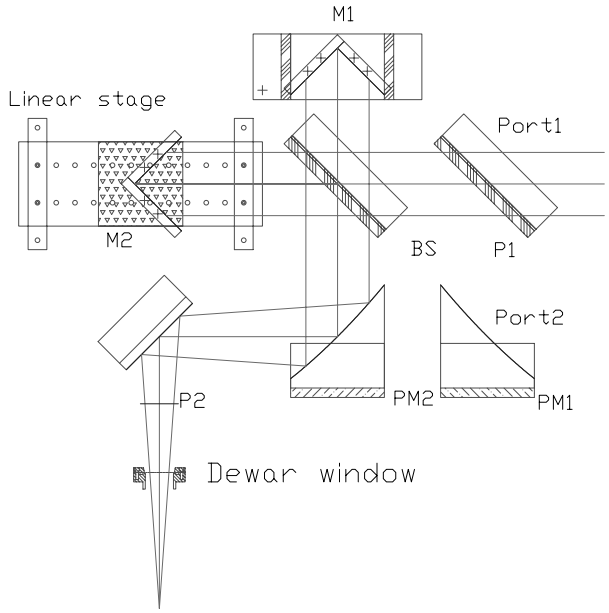

Figure 3. Fourier transform spectrometer layout. The incoming radition enters through port 1, which is modulated by a chopper. The optical components are the paraboidal collimating mirror PM1, the input polarizer P1, the wire-grid beam spliter BS,the fixed roof-mirror M1, the moving roof-mirror M2, the paraboidal focusing mirror PM2 and the output polarizer P2. The input polarizer P1 is tilted 45 degrees to provided two input ports.

The complete system is described according to figure 4. As explained above the incoming radiation is chopped to achieve a modulated signal that goes through the different mirrors and polarizers of the interferometer and

Table 1. Main parameters for different components of the INAOE FTS-MP.

Frequency range	∼215 GHz - 1 THz
Max. resolution (unapodized)	0.5 GHz
Grid period/wire diameter	75 μm/25 μm
Operating mode	continuous/chopped signal
Chopping frequency	3.8 Hz
Translation stage velocity	40 μm/s
Max. travel	180 mm
Detector	NTD Ge composite bolometer
NEP_{bol}	1.73 $\times 10^{-14}$ W $Hz^{-1/2}$
Winston Cone, F/#	4.74
FTS clear aperture	$\sim$ 70 mm
Control/acquisition system	x86, Win NT, LabView 6i

at the output port the signal enters the zotefoam window of the cryostat and it is feed to the bolometer with a Winston horn. The incident radiation on the detector produces a change on temperature on the bolometer thermistor which produces a change in its resistance, because the bolometer is current bias this produces as an output a changing voltage which is readout with a pair of JFETs.

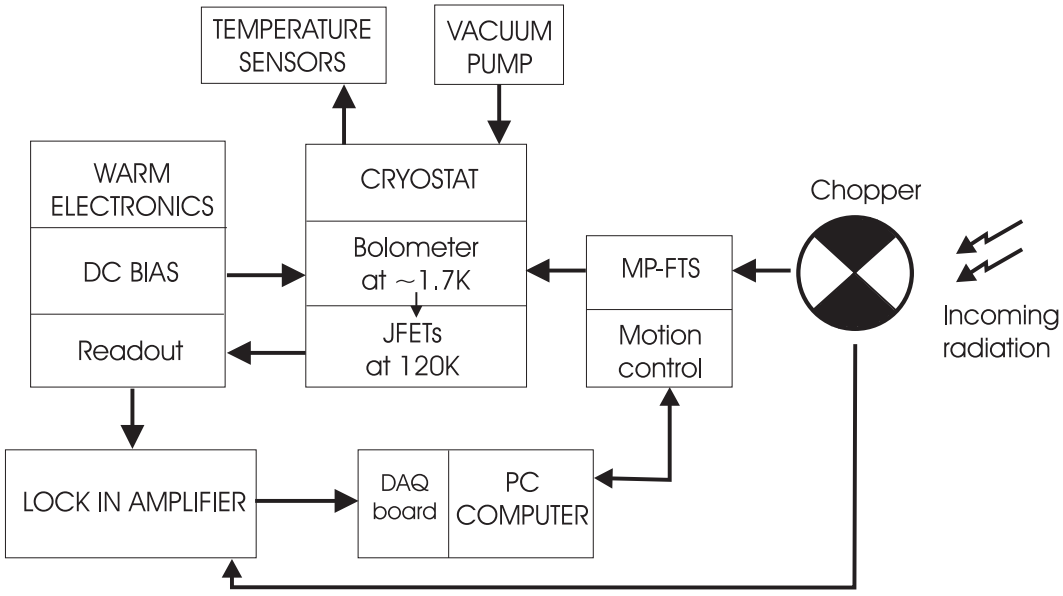

Figure 4. MP-FTS block diagram of the different system components.

On a second stage of amplification, the signal is sent to a room temperature instrumentation amplifier which increases the signal up to 10 times. The output signal from the amplifier is sent to a lock in amplifier to demodulate it and to reject noises different from the frequency at which the signal was initially modulated. At this point is possible to recover an interferogram, which is a signal in the time domain. Finally the interferogram is digitized using a DAQ board from National Instruments, with acquisition software written in Labview 6i,

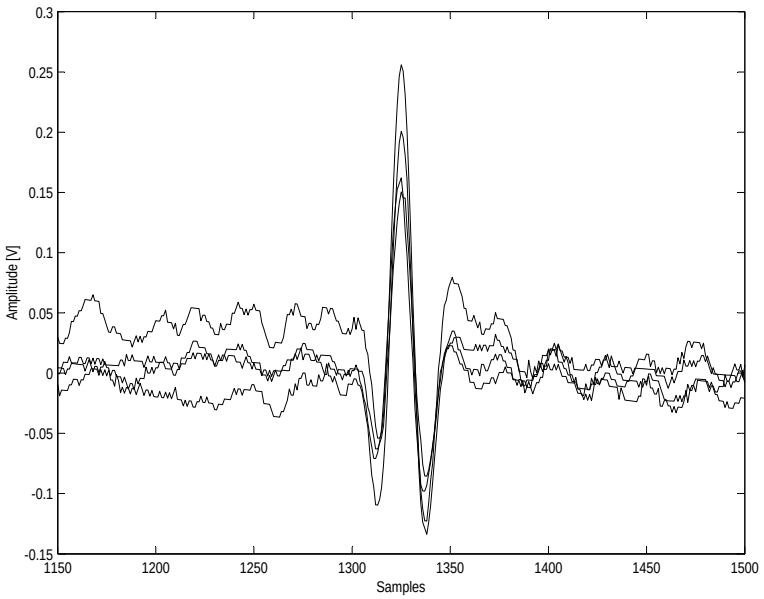

Figure 5. Several interferograms used for averaging. Source of 300 K chopped against liquid nitrogen reference load.

and running under a Windows NT platform on a PC computer. Post-processing of the inreferograms allows to recover spectrums and calibrate them in frequency and in phase.

4. RESULTS

The interferogram recorded $I(t)$ contains information about the radiant energy at given frequency ν. If the interferometer is illuminated by a polychromatic source, all the wave trains will be registered at the detector. The interferogram signal will be

$$I(t) = \int_{\sigma 1}^{\sigma 2} I(\sigma) cos(4\pi\sigma\upsilon t) d\sigma, \tag{1}$$

where $I(\sigma)$ is the spectrum of the polychromatic source passing through the interferometer and υ is the velocity of the linear stage. Changing the integral limits to $-\infty$ to $+\infty$ and substituting t by $\delta/2\upsilon$ we obtain the Fourier transform of $I(\sigma)$. If the interferogram is symmetric about the central fringe (i.e. zero path difference), the spectrum of the source can be found by taking the inverse Fourier transform

$$I(\sigma) = \int_{-\infty}^{+\infty} I(\delta) cos(2\pi\sigma\delta) d\delta. \tag{2}$$

Figure 5 shows a set of interferograms acquired in the first test at lab. The set was recorded in an interval of 30 min, for maximum mirror displacement of 150 mm. A source of 300 K was modulated against the cold load. The signal is demodulated by a lock-in amplifier while the linear stage slowly scan the interferogram. The signal from the lock-in amplifier is the difference in power between the sky brightness temperature and the cold load brightness temperature. An important parameter used to acquire correctly the inteferogram is the time constant of the lock-in which should be determined correctly to obtain the correct signal to noise ratio. The time constant is selected to be the half the period of the sampling rate. From figure 5 we observe that the shape of the secondary fringes is repetitive. The above is clear indication of no artifacts within the interferograms.

Figure 6 shows the spectrum computed from the one of the interferograms showed in figure 5. A non symmetric interferogram will introduce artifacts in the final spectrum computed, limiting the accuracy of the spectral information. The are several causes of phase errors in the FTS system, for example misalignments on

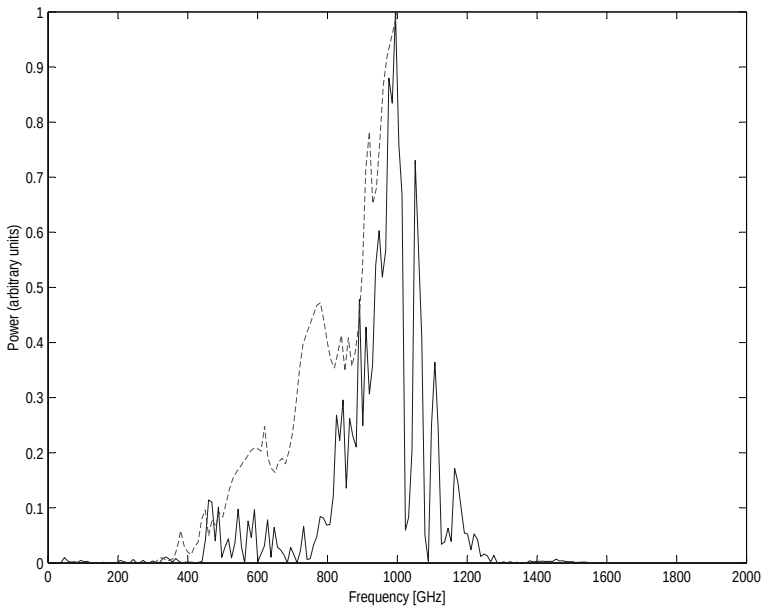

Figure 6. Phase corrected spectrum using the Mertz method. The solid line is the normalized spectrum of the average of the interferograms shown in the figure 5. The dashed line is the normalized synthetic spectrum for source of 77 K.

the optics, offsets due to electronic readout, optical path sampling errors, beam splitter dispersion and distortion introduced by variations in translation stage. Ideally a spectrum computed from an ideal FTS should have no imaginary component and therefore have zero phase. Figure 7 shows the phase spectrum obtained from the FTS-MP, which is a probe of possible misalignment in the optical elements mainly. Those phase errors can be corrected using the Mertz method after accurate process of alignment. The instrumental phase is determined taking a small symmetric sample about the central fringe and Fourier transforming. The result is a low-resolution, high signal-to-noise spectrum computed, which is normalized to produce the phase spectrum. Using the real and the imaginary part of the high signal-to-noise computed spectrum, the phase is obtained as

$$\theta(\sigma) = arctan\frac{\Im(\sigma)}{\Re(\sigma)}, \tag{3}$$

where $\theta(\sigma)$ is the phase of the input radiation. The Fourier transformed spectrum from the the full interferogram can be expressed as

$$I(\sigma) = A(\sigma)exp(i\theta(\sigma)), \tag{4}$$

where A(σ) is the amplitude. The product of the complex conjugate of this phase spectrum $exp(-i\theta(\sigma))$ and the spectrum computed from the full interferogram $I(\sigma)$, is the phase-corrected spectrum computed of the source $A(\sigma)$.

5. CONCLUSIONS

The FTS-MP has been built and tested in the laboratory. The Martin-Puplett optical configuration used for the FTS allows a quite simple design and fast implementation with limited resources. The FTS-MP is the first system in which was applied our detection bolometric system. The sensitivity of the sensor is improved by cooling down up to 1.49 K. The above sacrifices the hold time of the dewar, such that is not practical for a long term experiment. A new sensor will be required in order to take advantage of the cryogenic system at operating temperature of 4.2 K. The next objective is to build an assisted-system that allows a long-term site evaluation program to establish the time statistics of the atmospheric characteristics.

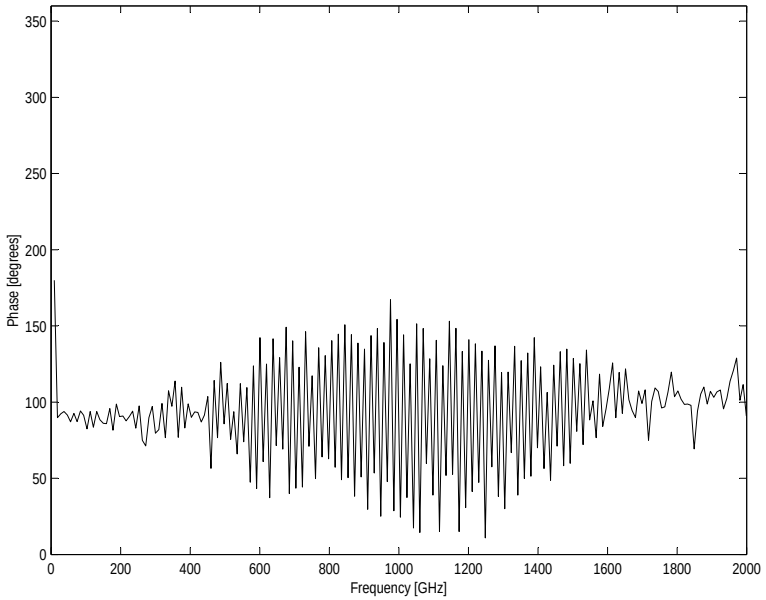

Figure 7. Uncorrected phase spectrum from the average of the interferograms shown in figure 5

ACKNOWLEDGMENTS

We thank Mark Devlin from the University of Pennsylvania and Grant Wilson from the University of Massachusetts for their valued comments and suggestions for this work. This project is supported by the Instituto Nacional de Astrofísica Optica y Electrónica grants and by CONACyT grants 129107 and 118617.

REFERENCES

1. V. Torres, V. Davydova, L. Carrasco, and I. Guzmán, "Evaluation of the long term behaviour of sites for mm-wavelength radioastronomy: the quest for a site for the large millimeter telescope," *Technical report. INAOE/GTM, Tonantzintla, Puebla.* **Dic.97**, 1997.
2. J. Estrada, J. Meza, and A. Torres, "Mediciones de opacidad atmosferica en el volcan sierra negra," *Technical report. INAOE/GTM, Tonantzintla, Puebla.* **RT0545**, 2002.
3. D. Ferrusca, M. Velázquez de La Rosa, D. H. Hughes, M. Devlin, and D. Swetz, "A polarizing Fourier Transform Spectrometer to characterize millimeter-wavelength filters and measure the atmospheric opacity," in *Revista Mexicana de Astronomia y Astrofisica Conference Series*, A. M. Hidalgo-Gámez, J. J. González, J. M. Rodríguez Espinosa, and S. Torres-Peimbert, eds., pp. 239–240, Dec. 2005.
4. J. Mather, "Bolometer noise: nonequilibrium theory," *Appl. Opt.* **21**, p. 1125, 1982.
5. P. L. Richards, "Bolometers for infrared and millimeter waves," *J.Appl.Phys.* **76**, p. 1, 1994.
6. E. E. Haller, K. M. Itoh, J. W. Beeman, W. L. Hansen, and V. I. Ozhogin, "Neutron transmutation doped natural and isotopically engineered germanium thermistors," *Instrumentation in Astronomy VIII* **2198**(1), pp. 630–637, SPIE, 1994.
7. W. Welford, *The optics of nonimaging concentrators, light and solar energy*, Academic Press, N. Y., 1978.
8. D. H. Martin, "Polarizing martin-puplett interferometric spectrometers for the near and submillimeter spectra," in *Infrared and Millimeter Waves, Vol. 6: Systems and Components*, K. E. Button, ed., pp. 66–148, Academic Press, New York, 1982.